Journal of Inflammation Research

Dovepress
Taylor & Francis Group

Open Access Full Text Article

ORIGINAL RESEARCH

Mechanisms of Acetate in Alleviating SETDB1-Linked Neuroinflammation and Cognitive Impairment in a Mouse Model of OSA

Zhan Zhao[1,*], Li Xiang[1,*], Jau-Shyong Hong[2], Yubao Wang[1], Jing Feng[1]

[1]Respiratory Department, Tianjin Medical University General Hospital, Tianjin, 300052, People's Republic of China; [2]Neurobiology Laboratory, National Institute of Environmental Health Sciences, National Institutes of Health, Research Triangle Park, Durham, NC, 27709, USA

*These authors contributed equally to this work

Correspondence: Yubao Wang; Jing Feng, Respiratory Department, Tianjin Medical University General Hospital, Tianjin, 300052, People's Republic of China, Email yubaowang2020@hotmail.com; tmugh_fj@tmu.edu.cn

Background: Microglia-mediated neuroinflammation is crucial for obstructive sleep apnea (OSA)-induced cognitive impairment. We aimed to investigate roles of acetate (ACE) and SET domain bifurcated histone lysine methyltransferase 1 (SETDB1) in neuroinflammation of OSA.

Methods: After C57BL/6J mice were exposed to OSA-associated intermittent hypoxia (IH) or normoxia for four weeks, the composition of the gut microbiota (GM) and the levels of serum short-chain fatty acids (SCFAs) were measured by 16S rRNA and GC-MS methods, respectively. To assess the effect of ACE on IH mice, glyceryl triacetate (GTA) was gavaged in IH-exposed mice and the cognitive function, microglial activation, and hippocampal neuronal death were examined. Moreover, ACE-treated BV2 microglia cells were also utilized for further mechanistic studies.

Results: IH disrupts the gut microbiome, reduces microbiota-SCFAs, and impairs cognitive function. Gavage with GTA significantly mitigated these cognitive deficits. Following IH exposure, we observed substantial increases in SETDB1 both in vivo and in vitro, along with elevated levels of histone H3 lysine 9 trimethylation (H3K9me3). Genetic or pharmacological inhibition of SETDB1 in microglia led to decreased induction of proinflammatory factors, as well as reduced reactive oxygen species (ROS) generation. Mechanistically, SETDB1 was found to upregulate the transcription factors p-signal transducer and activator of transcription 3 (p-STAT3) and p-NF-κB. In vitro, ACE supplementation effectively repressed high SETDB1 and H3K9me3 levels, thereby inhibiting microglial pro-inflammatory responses induced by IH. In vivo, ACE supplementation significantly reduced hippocampal levels of p-STAT3, p-NF-κB, and pro-inflammatory cytokines while also protecting neuronal integrity.

Conclusion: This study provides the first evidence that H3K9 methyltransferase SETDB1 promotes microglial pro-inflammatory response distinct from its previously shown role in macrophages. Our findings also identify ACE supplementation as a promising dietary intervention for OSA-related cognitive impairment with SETDB1 serving as both a mechanistic biomarker and potential therapeutic target.

Keywords: acetate, neuroinflammation, OSA, SETDB1, NF-κB, STAT3

Introduction

Obstructive sleep apnea (OSA) is a condition marked by frequent blockages of the upper airway that cause intermittent hypoxic stress (IH), impacting approximately one in seven people globally.[1] Increasing evidence suggests that OSA might be closely linked to cognitive deficits and neurodegenerative conditions through the activation of neuroinflammatory signaling pathways,[2] however, the underlying mechanisms remain enigmatic.

Microglia, the primary innate immune cells of the central nervous system (CNS), drive neuroinflammation by releasing neurotoxic factors, including interleukin-1β (IL-1β), tumor necrosis factor-alpha (TNF-α), and toxic superoxide free radicals.[3] Both exogenous and endogenous stress factors and damage signaling pathways can lead to microglial

Received: 16 December 2024
Accepted: 26 April 2025
Published: 7 May 2025

activation, resulting in neuronal damage.[4] For instance, the NOD-like receptor protein 3 (NLRP3) inflammasome can drive neuroinflammation through extracellular secretion of caspase-1 and IL-1β. Our previous study demonstrates that chronic inflammation relies on NLRP3-IL-1β signaling, promoting α-synuclein aggregation in the hippocampus and substantia nigra.[5] Under these pathological conditions, the activation and nuclear translocation of NF-κB induces the transcription of NLRP3 and pro-IL-1β[6] and modulates the NLRP3-IL-1β pathway to progressively amplify inflammatory responses, thus exacerbating CNS damage.[7] Exposure to IH can also activate microglia, resulting in varying degrees of neuronal damage in cognition-associated brain regions. Studies show that OSA can provoke microglial activation, increase NF-κB and pro-inflammatory factors' expression, and enhance oxidative stress (OS), leading to the loss of hippocampal neurons, and ultimately contributing to cognitive deficits.[8]

IH, a pathological hallmark of OSA, induces vicious cycles of hypoxia/reoxygenation in the intestinal microbiota, which can alter gut microbiota (GM) diversity and impact levels of short-chain fatty acids (SCFAs), key metabolites, and secondary signaling molecules produced by the microbiota.[9] SCFAs, including acetate, propionate, and butyrate, play crucial roles in maintaining gut and overall health.[10] Research has shown that ACE, in particular, can restore microglial function and modulate microglial activity in response to neurodegenerative stresses, whereas propionate and butyrate do not have the same effect.[11] At present, the effect of ACE on the central nervous system remains unclear in OSA. Glycerol triacetate (GTA) as a prodrug of ACE been approved by the US Food and Drug Administration (FDA) as a safe food additive and shows potential for clinical translation if proven effective against OSA-induced cognitive impairment.

Histone methylation, a fundamental epigenetic regulatory mechanism, can either enhance or suppress inflammatory responses depending on the specific modification involved. SET domain bifurcated histone lysine methyltransferase 1 (SETDB1), a histone methyltransferase, specifically targets lysine 9 on histone H3 to produce the transcriptional repressor trimethylated H3K9 (H3K9me3).[12] SETDB1 in macrophage shows inhibition of peripheral inflammatory responses to Lipopolysaccharide (LPS) in both macrophage cell line and mouse model.[13] However, its role in microglia is still unclear. Currently, histone methyltransferases have attracted increasing attention as an emerging therapeutic target.[14] Therefore, as a methyltransferase, SETDB1 has also drawn our special attention regarding its effect as a target for therapeutic intervention in OSA-related neuroinflammatory responses.

In this study, we utilized an OSA model of IH in mice, along with GTA for animal study and ACE for cell cultures as acetate supplements, to explore the role of SETDB1 and ACE in IH-induced neuroinflammation and cognitive deficits. Surprisingly, increased SETDB1 level promotes neuroinflammation via upregulating the transcription factors p-STAT3 and p-NF-κB, which is different from its function in macrophages. ACE supplementation decreases SETDB1 and H3K9me3 levels, inhibiting IH-induced neuroinflammation and alleviating cognitive deficits in OSA models. This study is the first to show that SETDB1 plays a crucial role in promoting neuroinflammation in microglia and suggests that ACE may mitigate OSA-related neuroinflammation through its effects on SETDB1.

Materials and Methods

Animals and Exposures

Male C57BL/6J mice (10-wk-old, 18–22g weight) were obtained from Beijing HFK BioTechnology Co. Ltd. In this study, only male mice were used to avoid estrous cycle-related hormonal effects on inflammation and metabolism.[15] Mice were housed in a specific pathogen-free facility at 22±1°C and 50±10% humidity, with 5 mice per cage (36×20×14 cm). Sterilized bedding was changed twice weekly. They had free access to a standard rodent diet and sterilized tap water throughout the study. For one week, all mice were housed in a 12h light/dark cycle to adapt to the experimental environment. Mice were randomly distributed into the negative control (NC), GTA, IH, and IH+GTA groups. The IH and IH+GTA groups' mice were exposed to 30 cycles/h for 8 h/day for 4 wks (minimum 5% O_2 for 30s, maximum 21% O_2 for 90s). The NC and GTA mice were kept under normoxic conditions. The GTA and IH+GTA groups received GTA gavage (2 g/kg/day) under IH or normoxic conditions. The control group received equivalent volumes of the solvent by gavage. GTA (#G810356-100 g, Mackin Biochemical Technology Co. Ltd, China) was prepared in 0.5% sodium carboxymethyl cellulose (CMC-Na) dissolved in double-distilled water. GTA was selected as the ACE donor based on its high capacity for penetrating brain cells and effectively increasing the brain ACE level by more than 15-fold

within one hour after administration.[16] Next, we collected mouse feces and conducted behavioral tests after treatments. Mice were anesthetized by an intraperitoneal (i.p). injection of 10% chloral hydrate (0.3 mL/100 g) for blood collection and sacrifice. Mice were either preserved as whole-brain specimens or had their hippocampal tissue carefully dissected and stored at −80°C for subsequent analyses. The experimental timeline, including all critical interventions and sampling time points, is presented in Figure 1A.

16S rRNA Sequencing

Fecal samples (0.25 g/sample) were processed for total microbial DNA isolation using the EZNA Soil DNA kit (#M5635, Omega Biotek, USA), following the manufacturer's protocol. The 16S rRNA gene was amplified using primers: 338F: 5′-ACTCCTACGGGAGGCAGCAG-3′ and 806R: 5′-GGACTACHVGGGTWTCTAAT-3′ targeting the V3-V4 hypervariable regions. The raw reads were screened and restructured using QIIME2 (version 2019.4). A 97% cutoff was set for indexing operational taxonomic units (OTUs). Any OTU with values lower than 0.001% of the total sequencing amount was eliminated. This abundance matrix was applied to rare OTUs for α and β diversity analyses.

Serum Metabolomics

Blood samples were centrifuged at 3500 rpm for 15 min at 4°C, and the supernatant was collected for GC-MS analysis. Serum samples (150 μL) were incubated at −20°C for 20 min, followed by centrifugation and drying. The pellet was dissolved in methoxamine hydrochloride pyridine solution (80 μL,15 mg/mL) by shaking at 30°C for 90 min. Then, 20 μL of n-Hexane and 50 μL of BSTFA were added to the solution and incubated at 70°C for 20 min. After that, mixtures were kept at room temperature for 30 min, followed by GC-MS analysis on the TRACE-1310 GC analyzer (Thermo Fisher Scientific, USA). Mass spectrometric detection of serum SCFA concentrations was performed on ISQ LT (Thermo Fisher, USA).

Behavioral Tests

Y-Maze Test

Y-maze has three arms – A (40 cm), B (40 cm), and C (40 cm). The ANY-maze software (version 7.40, Stoelting Co., IL, USA) was used to record and analyze spontaneous alternation rates. The starting point of movement measurement was set at the end of the A-arm, allowing the animal to move freely for 5 min. A camera placed above the maze recorded the entire movement trajectory and pattern. The percent alternation behavior was calculated as follows: number of successful alternations/((total number of arms entries – 2) ×100).

Morris Water Maze Test

The Morris Water Maze (MWM) test was performed in an opaque cylindrical water tank, having a diameter of 134.5 cm and a depth of 40 cm, at 20–24°C. All sessions were also recorded and analyzed using ANY-maze software. A circular escape platform, measuring 10 cm in diameter, was submerged 1cm below the water surface in one of the four quadrants. Mice underwent a training period of 5 days, during which they were placed in the water facing the wall and given 120 s to locate the platform. If a mouse failed to find the platform within this time, it was gently guided to the platform and allowed to remain there for 10s. On the 6th day of testing, the escape platform was removed, and the mouse was given 120 s to search for the location where the platform had been. A camera automatically recorded the escape latency (ie, the time spent in the target quadrant), as well as the total swimming distance.

Cell Culture

Mouse BV2 microglia (Zhongqiaoxinzhou Biotech, China) were cultured in Dulbecco's modified Eagle medium (DMEM, # C11965500BT, Thermo Fisher, USA) complete medium, supplemented with 10% fetal bovine serum (FBS, #164210-50, Wuhan Pricella Biotech Co. Ltd, China), and 100U/mL penicillin and 100 μg/mL streptomycin solution (#P1400, Solarbio, China) at 37°C in a 5% CO_2 humidified incubator. At about 80% confluency, cells were passaged and seeded into 6-well plates for the experiment.

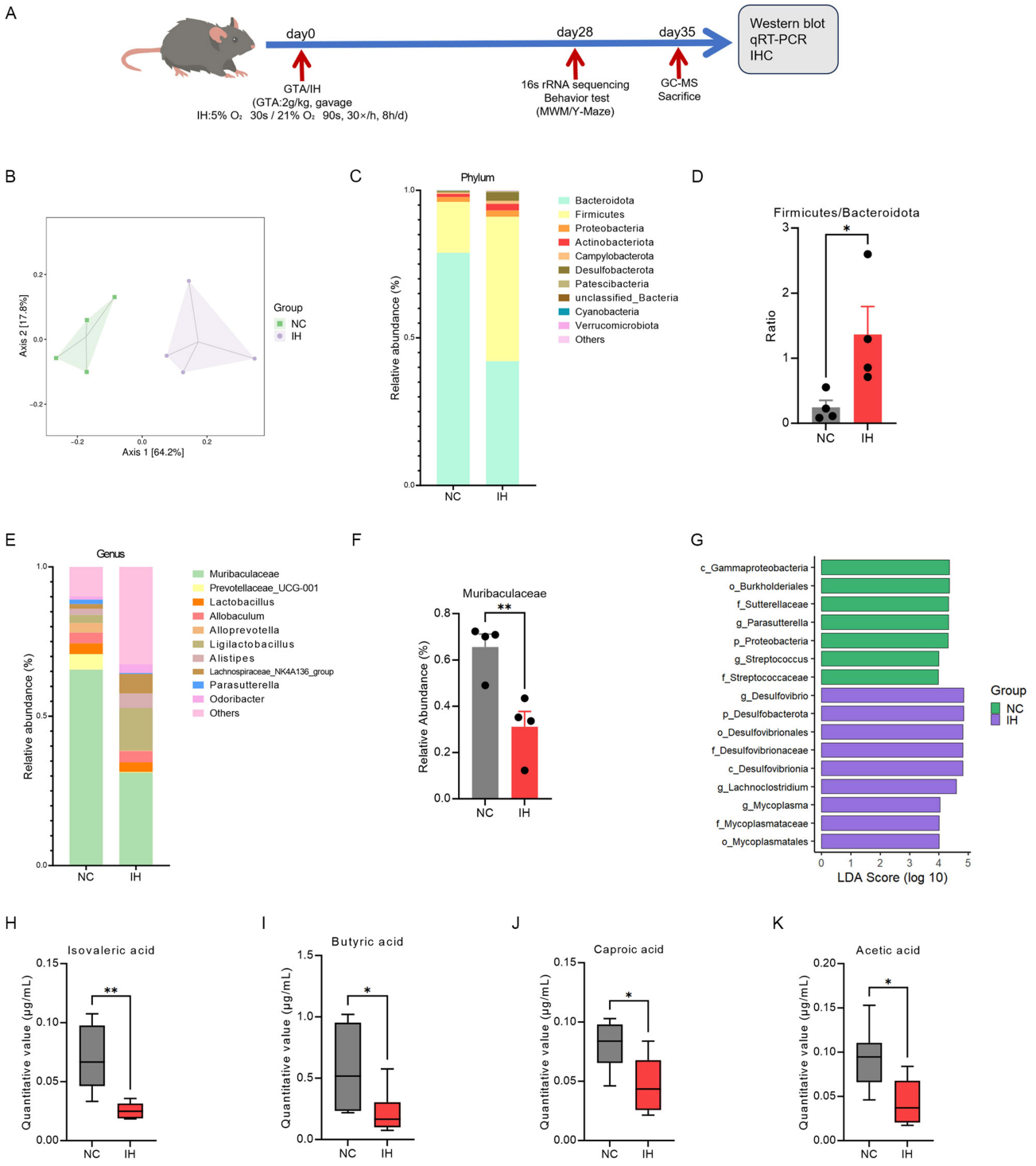

Figure 1 IH disturbed the gut microbiota (GM) and reshaped the composition of short-chain fatty acids (SCFAs). (**A**) The experiment's timeline. (**B**) Principal coordinates analysis (PCoA) of fecal microbiota from negative control (NC) and intermittent hypoxia (IH) group (n = 4 per group). (**C**) GM composition at the Phylum level. (**D**) The ratio of phylum *Firmicutes*/*Bacteroidetes* (F/B). (**E**) GM composition at the Genus level. (**F**) Comparison of abundance of *Muribaculaceae* between NC and IH groups with n = 4. (**G**) Histogram of LDA was used to analyze the abundance of GM to identify microorganisms with significant differences between the NC and IH groups. (**H-K**) Serum samples were analyzed by gas chromatography-mass spectrometry (GC-MS) to show that IH changes the concentration of SCFAs including isovaleric acid, butyric acid, caproic acid, acetic acid (n = 6 per group). *$p < 0.05$, **$p < 0.01$. p values are based on the Student's t-test.

Cell Treatments

The cells were quickly placed in a gas delivery system consisting of a 1.8L cell culture chamber that controls and monitors O_2, CO_2, and pH while maintaining stable temperature and humidity. They were then exposed to different oxygen concentrations to simulate repeated respiratory pauses after adding ACE dissolved in phosphate-buffered saline (PBS) (20 mM, #S7545, Sigma-Aldrich, USA) or SETDB1 inhibitor TD dissolved in dimethyl sulfoxide (DMSO) (5 μM, #HY141539, MedChemExpress, USA) with controls receiving vehicle-only treatments. For IH exposure, cells were exposed to a cycle of low oxygen for 30s (1.5% O_2) and reoxygenation for 90s (21% O_2) for 8 h. Control cells were maintained in a normoxic environment. The exposure time for each group was 24 h.

Transfection of Small-Interfering RNA (siRNA)

SiControl (scrambled siRNA) or siSETDB1 (GenePharma, China) was transfected in BV2 cells plated in 6-well plates using GP-Transfect Mate (#G04009, GenePharma, China), following the manufacturer's protocol. At 40 h post-transfection, the culture medium was replaced with a fresh, complete medium. Then IH exposure was performed for 8 h and samples were collected for further analyses.

Real-Time Quantitative Polymerase Chain Reaction (qRT-PCR) Analysis

TRIzol method (#15596026, Invitrogen, USA) was used to extract total RNA from cell pellets and hippocampal tissue (about 20 mg per sample) with 1 μg of RNA used for cDNA synthesis. Complementary DNA (cDNA) was synthesized using HisyGo-RT Red SuperMix Kit (#RT101-01, Vazyme, China) and qRT-PCR was performed as described elsewhere.[8] The gene expression results were presented in fold changes normalized to the housekeeping control gene expression (β-actin) with ΔΔCT method.

Immunohistochemistry (IHC) and Immunofluorescence (IF)

For IHC analysis, brains were fixed in 4% paraformaldehyde (PFA) and embedded in paraffin blocks, then sectioned into tissue slices of 5 μm thickness. The tissue slices selected for IHC staining were from the hippocampal CA1 subfield and and dentate gyrus (bregma −1.70 to −2.30 mm). After deparaffinization and gradient hydration, tissue sections were stained in hematoxylin (#G1004) and eosin (#G1001) solutions for 5 min and 20s, respectively, using an H&E kit (Servicebio, China). For Nissl staining, sections were stained with toluidine blue solution (#DK0020, Beijing Leigen Biotech, China) for 8 min. For IHC analysis using anti-Iba-1 antibody, brain sections were treated with 1% hydrogen peroxide solution, followed by a blocking solution. Primary antibody incubation was then performed overnight at 4°C using anti-Iba-1 antibody (1:100, #ab178846, Abcam, USA), whose specificity had been previously validated in same tissue and species.[17] Then it was washed twice with PBS, and incubated with goat anti-rabbit secondary antibody (1:200, #ab20571, Abcam, USA) for 1 h. Signals were captured using an NanoZoomer S210 (model: C13239-01, Hamamatsu Photonics K.K., Japan).

For IF, BV2 cells were fixed with 4% PFA for 30 min, washed twice with PBS, permeabilized with 0.1%Triton X-100 for 10min, blocked for 30 min, and incubated with specificity-validated anti-NLRP3[18] (1:200, #68102, Proteintech, China) and anti-SETDB1[19] (1:200, #ab107225, Abcam, USA) antibodies at 4°C overnight. The next day, anti-rabbit (#SA00013-2, Proteintech, China) or anti-mouse secondary antibodies (#SA00013-1, Proteintech, China) were added (1:200), amplified with Vectastain ABC reagents (#AK-6000, Vector Labs, USA), and visualized with 3.3'-diaminobenzidine (DAB, #12384, Sigma-Aldrich, USA). For ROS IF staining, the ROS Assay Kit (#S0033-1, Beyotime, China) was used. Samples were examined under a fluorescence microscope. (model: MC50-S, Guangzhou Mshot Photoelectric Technology Co., Ltd, China).

Western Blotting (WB)

Cells were lysed in RIPA Buffer (#P0013B, Beyotime, China) for 30 min on ice, followed by centrifugation at 12000 rpm at 4°C, and the supernatant was collected for WB. Around 20 mg of dissected hippocampal tissue per sample was homogenized in RIPA, as well. Histones were isolated using a Histone Extraction kit (#ab221031, Abcam, USA),

according to the manufacturer's instructions. Protein concentrations were measured by a BCA Kit (#23277, Thermo Fisher, USA). Equal amounts of protein (20 μg protein loaded per lane) were resolved in an SDS-PAGE and transferred onto polyvinylidene difluoride (PVDF) membranes. The membranes were blocked with 5% non-fat skimmed milk and incubated with respective primary antibodies overnight at 4°C: anti-H3K9me3 (1:1000, #19369S, CST, USA), anti-STAT3 (1:1000, #9139T, CST), anti-p-STAT3 (1:1000), anti-p-NF-κB (1:1000, #9145T, CST), anti-NF-κB (1:1000, # ab32536, Abcam), anti-SETDB1 (1:1000, # ab107225, Abcam), anti-NLRP3 (1:1000, #15101S, CST), anti-IL-1β (1:1000, #ab283818, Abcam), anti-TNF-α (1:1000, #ab183218, Abcam), anti-H3 (1:1000, #ab1791, Abcam). Next, membranes were probed with corresponding secondary antibodies for 1h. The SuperSignal West Pico Plus (#34580, Thermo Fisher) was used for signal readout in a developing instrument. ImageJ was used for quantitative image analysis.

Statistical Analysis

For 16S rRNA sequencing analysis, principal component analysis (PCA) was performed. Wilcoxon rank-sum test was used to compare microbial communities between the two groups. Non-parametric factorial Kruskal–Wallis sum-rank tests were used to analyze the LEfSe cladogram. Linear discriminant analysis (LDA) method evaluated the contribution of diverse microbiota across the groups. A Student's *t*-test was applied to two-group comparisons, while a one-way ANOVA was followed by the Bonferroni post hoc multiple comparison test to compare multiple groups. GraphPad Prism v10.00 was used for graph plotting and data analysis. P values ≤ 0.05 were considered statistically significant. Data was presented as the mean ± standard error mean (SEM).

Results

IH Perturbs GM Homeostasis and Reshapes the SCFA Composition

16S rRNA sequencing revealed GM profiles in NC and IH mice. In α diversity, IH exposure did not alter GM diversity compared to the NC group, according to Chao1, Shannon and Simpson indexes (Figure S1A–C). In β diversity, the IH group showed significantly different principal components than the NC group (Figure 1B). At the Phylum level, IH stimulated a higher growth of *Firmicutes* while impacting *Bacteroidate*s growth (Figure 1C). The *Firmicutes* to *Bacteroidetes* (F/B) ratio is considered a biomarker to evaluate the pathological status of GM,[20] such that an increased F/B ratio indicates the depletion of SCFA-producing GM populations.[21] We found a significant increase in the F/B ratio after IH exposure (Figure 1D), suggesting GM imbalance and altered levels of SCFA. At the Genus level, *Muribaculaceae* were decreased by IH treatment (Figure 1E) with $p = 0.0073$ (Figure 1F). *Muribaculaceae*, an intestinal probiotic, produces important SCFAs, such as ACE, propionate, and butyrate by fermenting dietary fiber. The differential microbial populations from Phylum to Genus levels between the two groups are summarized using LEfSe LDA (Figure 1G). Notably, *Desulfovibrio* appeared as a marker strain in the IH group. Previous studies showed a negative correlation between the abundance of *Desulfovibrio* and the clinical status of Alzheimer's patients.[22] Moreover, *Desulfovibrio* is known to be associated with reduced fecal levels of SCFAs.[23] These results suggest that IH could disturb the GM homeostasis, affecting the physiological levels of important SCFAs. Next, we determined the composition of SCFAs in serum samples. Among the seven SCFAs, IH effectively decreased levels of isovaleric ($p = 0.0034$), butyric ($p = 0.0494$), caproic ($p = 0.0250$), and acetic acids ($p = 0.0196$) (Figure 1H–K). There were no significant changes in levels of isobutyric, valeric, and propionic acids (Figure S1D–F).

GTA Alleviates Cognitive Deficits in IH-Affected Mice

MWM and Y-maze tests were employed to assess the effect of GTA on the IH-exposed mice behavior. In the Y-maze test, IH mice presented significantly reduced spontaneous alternation rates compared to NC mice with $p = 0.0109$, which were rescued by GTA treatment (Figure 2A and B). The number of arm entries was similar across all four groups, suggesting that each group had comparable motor abilities (Figure 2C). The data demonstrated that GTA could mitigate the spatial working memory deficits induced by IH in mice. To further explore GTA's effects on learning and spatial memory, we conducted the MWM test. No significant differences in swimming speeds were observed among the groups (Figure 2D), indicating that GTA and IH exposure did not affect motor ability. IH mice took longer to locate the platform compared to

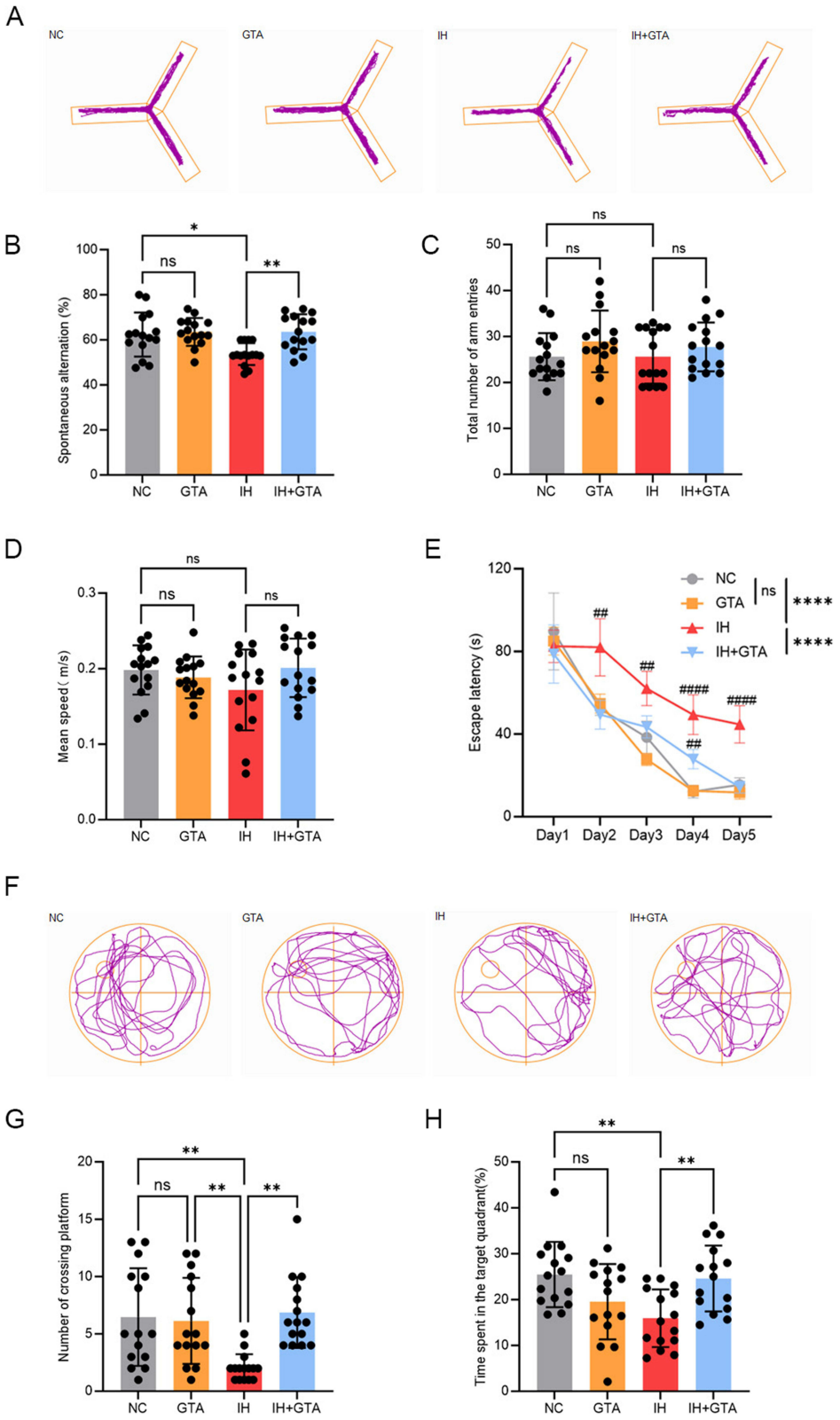

Figure 2 Behavioral tests assessing the effect of glyceryl triacetate (GTA) on cognitive deficits in IH-exposed mice. (**A**) Representative movement trajectories in the Y-maze test. The spontaneous alternations (**B**) and total number of arm entries (**C**) in the Y-maze test. (**D**) Swimming speed in the Morris water maze, with no significant differences detected. (**E**) Spatial learning ability assessed by escape latency in the Morris water maze. (**F**) Representative swimming trajectory after removal of the target platform. Memory ability was evaluated by the number of (**G**) crossings and (**H**) time spent in the target quadrant. n = 15 per group. *$p < 0.05$, **$p < 0.01$ and ****$p < 0.0001$. $^{\#\#}p < 0.01$ and $^{\#\#\#\#}p < 0.0001$ versus negative control (NC) group, ns = not significant. The data were analyzed with one-way ANOVA.

https://doi.org/10.2147/JIR.S510690

controls. And IH mice exhibited longer escape latency than controls on last four trails. However, the IH+GTA group showed a notably shorter escape latency during training ($p < 0.0001$ versus IH group), indicating that GTA improved learning impairments caused by IH (Figure 2E). Upon removal of the target platform, the swimming trajectories of these mice were changed (Figure 2F). The IH+GTA group exhibited a significant increase in both the number of platform crossings ($p = 0.0010$) and the duration of time spent in the target quadrant ($p = 0.0095$), compared to the IH group, demonstrating that GTA attenuates IH-induced memory function loss (Figure 2G and H).

ACE Supplementation Restores the Normal SETDB1 Level in IH-Microglia

Following our observation that GTA alleviates cognitive decline associated with IH in mice, we investigated the underlying mechanisms. We discovered that IH treatment significantly increased the expression of SETDB1 in microglia compared to the control group with $p = 0.0304$ (Figure 3A and B). After administering GTA via gavage, we found that SETDB1 expression was notably reduced in the brains of IH mice (Figure 3A and B). SETDB1, a histone lysine methyltransferase, is crucial for the formation of H3K9me3 from H3K9. WB analysis revealed a decrease in H3K9me3 levels in the IH+GTA group compared to the IH group (Figure 3C), with quantification shown in Figure 3D ($p = 0.0319$). This reduction supports GTA's role in inhibiting the increased SETDB1 levels following IH exposure. Additionally, in BV2 cells, ACE treatment significantly inhibited the high SETDB1 and H3K9me3 levels induced by IH (Figure 3E–H). The number of SETDB1-positive cells was significantly higher in BV2 cells exposed to IH than in controls with $p = 0.0103$, but this difference was almost eliminated in the IH+ACE group (Figure 3I and J), suggesting that ACE supplementation effectively mitigates the SETDB1 elevation caused by IH.

Inhibition of IH-Induced Elevation of SETDB1 Reduces Microglial Inflammatory Responses to IH

To determine whether changes in SETDB1 are merely a consequence of physiological disorders or if they play a functional role in IH-mediated neuroinflammatory damage, we inhibited SETDB1 expression by treating with siControl or siSETDB1 (Figure 4A and B). We then assessed the impact on inflammatory factors at the protein level through WB analysis. IH treatment resulted in elevated TNF-α levels compared to the control group (Figure 4A–E). However, siSETDB1 treatment significantly reduced TNF-α levels in BV2 cells ($p < 0.0001$ versus IH group). Building on our previous research highlighting the NLRP3-IL-1β signaling pathway's role in chronic neuroinflammation, we also measured NLRP3 (Figure 4A–C) and IL-1β (Figure 4A–D), and observed similar reductions as with TNF-α. Additionally, using the SETDB1 inhibitor TD produced results consistent with those obtained through gene suppression. Compared to controls, IH treatment significantly increased mRNA levels of TNF-α (Figure 4F), IL-1β (Figure 4G), and NLRP3 (Figure 4H) in microglia, while pharmacological inhibition of SETDB1 with TD significantly suppressed these increases. At the protein level, TD treatment also substantially reduced IH-induced overexpression of TNF-α (Figure 4I and J), IL-1β (Figure 4I–K), and NLRP3 (Figure 4I–L). To further confirm SETDB1's effect on OS, we performed IF-based ROS staining in BV2 cells. We observed a significant increase in ROS-positive cells following IH treatment with $p < 0.0001$, but this increase was not present in the IH+TD group ($p = 0.0008$), which was similar to the controls (Figure 4M).

ACE Inhibits the Inflammatory Responses of BV2 Cells to IH

Our results indicated that ACE supplementation affected SETDB1 and that SETDB1 was involved in IH-induced neuroinflammatory responses. To further validate ACE's impact on CNS inflammation post-IH exposure, we conducted in vitro studies using cultured microglial cells. Our findings showed that IH treatment led to a significant increase in the mRNA levels of inflammatory factors TNF-α (Figure 5A) and IL-1β (Figure 5B). However, ACE treatment significantly decreased the expression of both inflammatory factors ($p < 0.0001$), while ACE alone did not alter the expression of TNF-α and IL-1β mRNA in these cells. Similar results were observed at the protein level (Figure 5D–F). Additionally, ACE effectively inhibited NLRP3, a key player in chronic inflammation. NLRP3 mRNA levels were significantly reduced in the IH+ACE group compared to the IH group with $p = 0.0009$ (Figure 5C), and WB analysis confirmed that

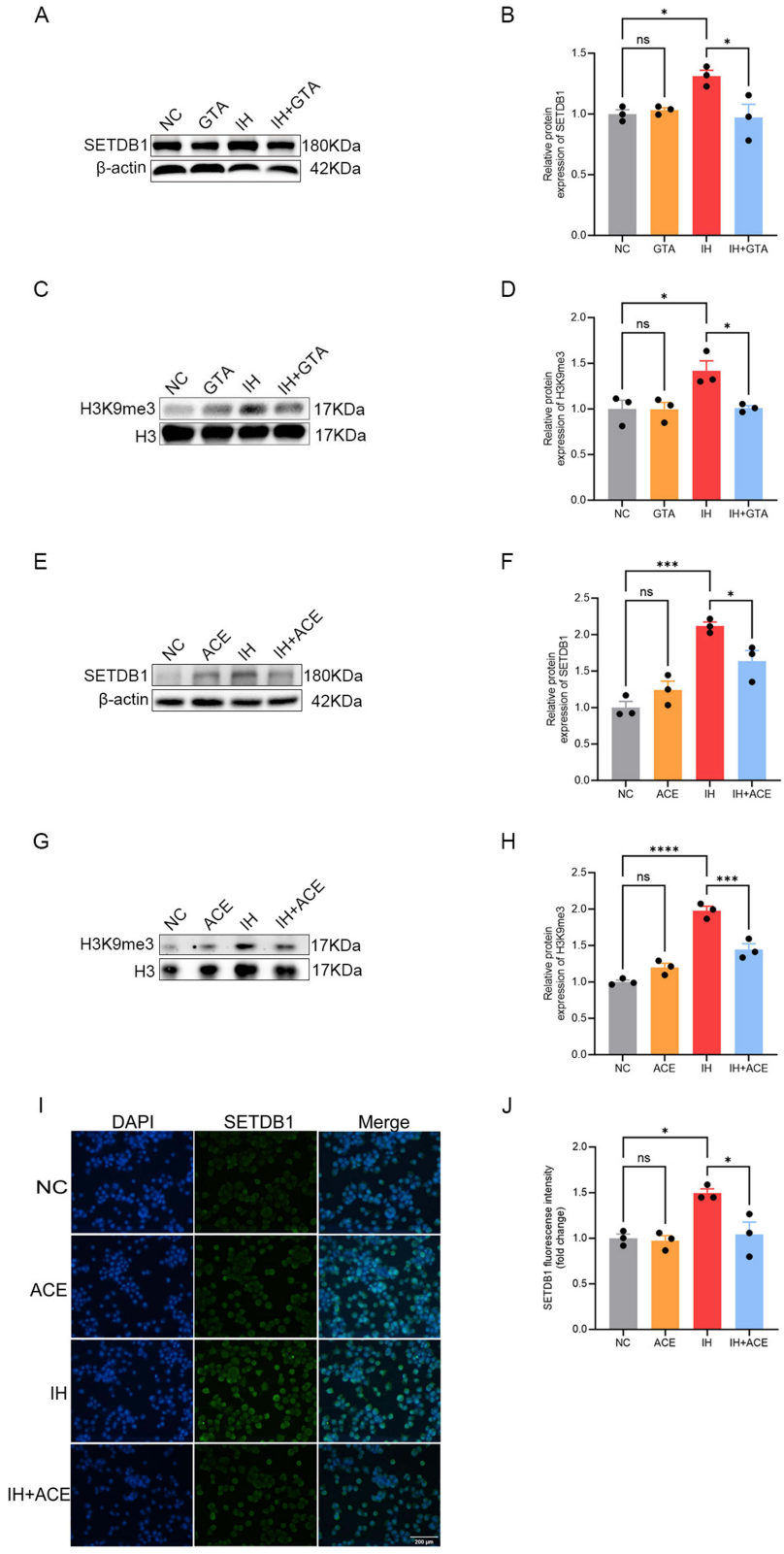

Figure 3 Acetate (ACE) supplementation inhibits the upregulation of SET domain bifurcated histone lysine methyltransferase 1 (SETDB1) induced by intermittent hypoxia (IH). Expression of proteins SETDB1 (**A**) and histone H3 lysine 9 trimethylation (H3K9me3) (**C**) in the brain of mice exposed to glyceryl triacetate (GTA) and/or intermittent hypoxia (IH) was analyzed by Western blot. *β*-actin and H3 served as a loading control. Quantification of SETDB1 (**B**) and H3K9me3 (**D**) protein levels. Protein levels of SETDB1 (**E**) and H3K9me3 (**G**) in BV2 cells treated with ACE and/or IH were analyzed by Western blot, with corresponding quantitative results in (**F**) and (**H**). (**I**) Representative immunofluorescence image of SETDB1 (green) in BV2 cells. Scale bars = 200 μm. (**J**) Quantification of SETDB1 intensity using ImageJ. n = 3 per group. * $p < 0.05$, *** $p < 0.001$ and **** $p < 0.0001$. ns = not significant. p values are based on one-way ANOVA.

https://doi.org/10.2147/JIR.S510690

result (Figure 5D–G). Furthermore, the population of NLRP3-positive cells was significantly lower in the IH+ACE group than in the IH group (Figure 5H).

Activated microglia-secreted ROS can exacerbate neuronal apoptosis in conjunction with TNF-α and IL-1β. We observed a marked reduction in ROS immunoreactivity in the IH+ACE group compared to the IH group with $p = 0.0117$ (Figure 5I). Overall, these in vitro studies demonstrate that ACE inhibits IH-induced neuroinflammation with effects similar to those observed with SETDB1 inhibition.

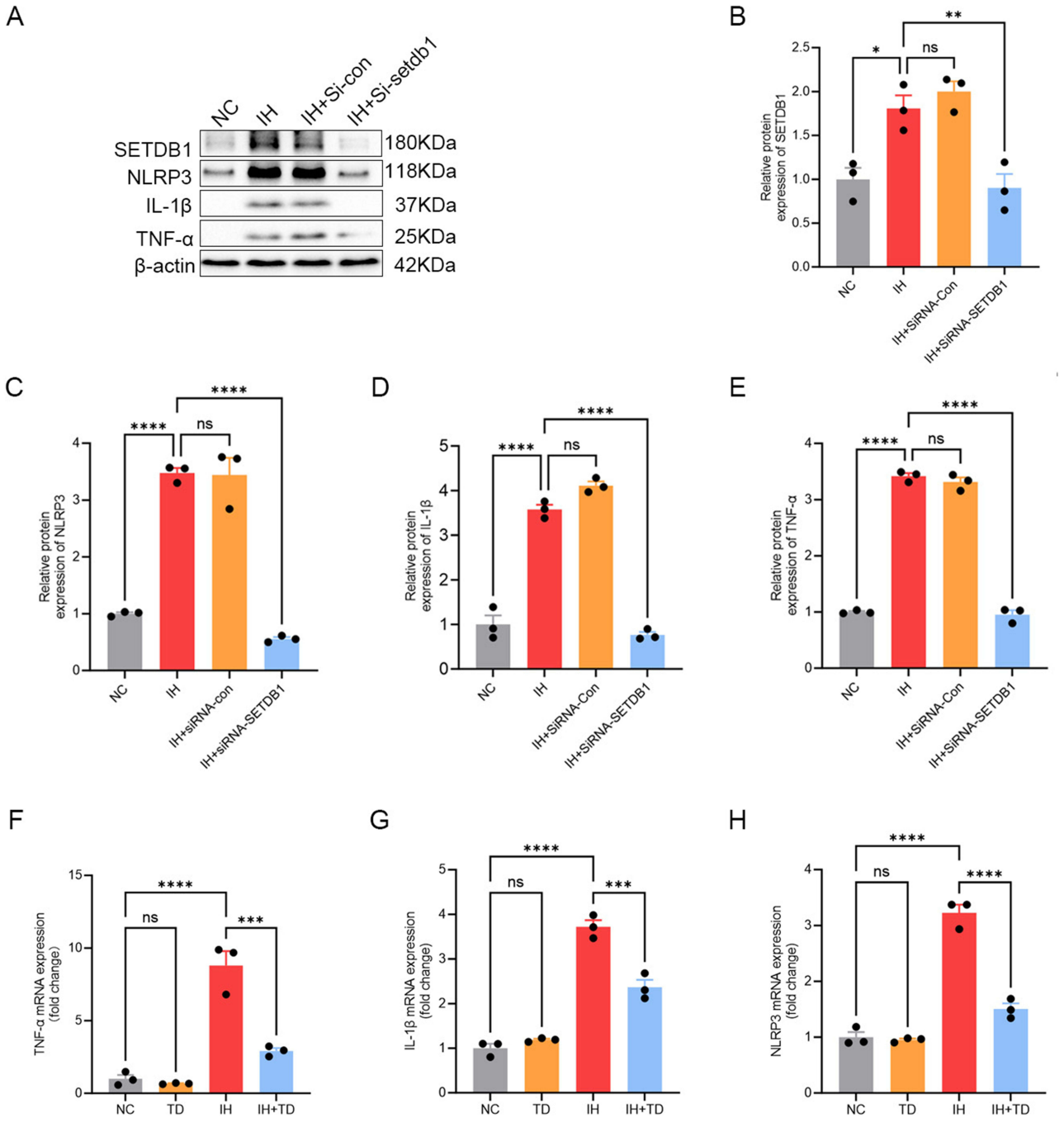

Figure 4 Continued.

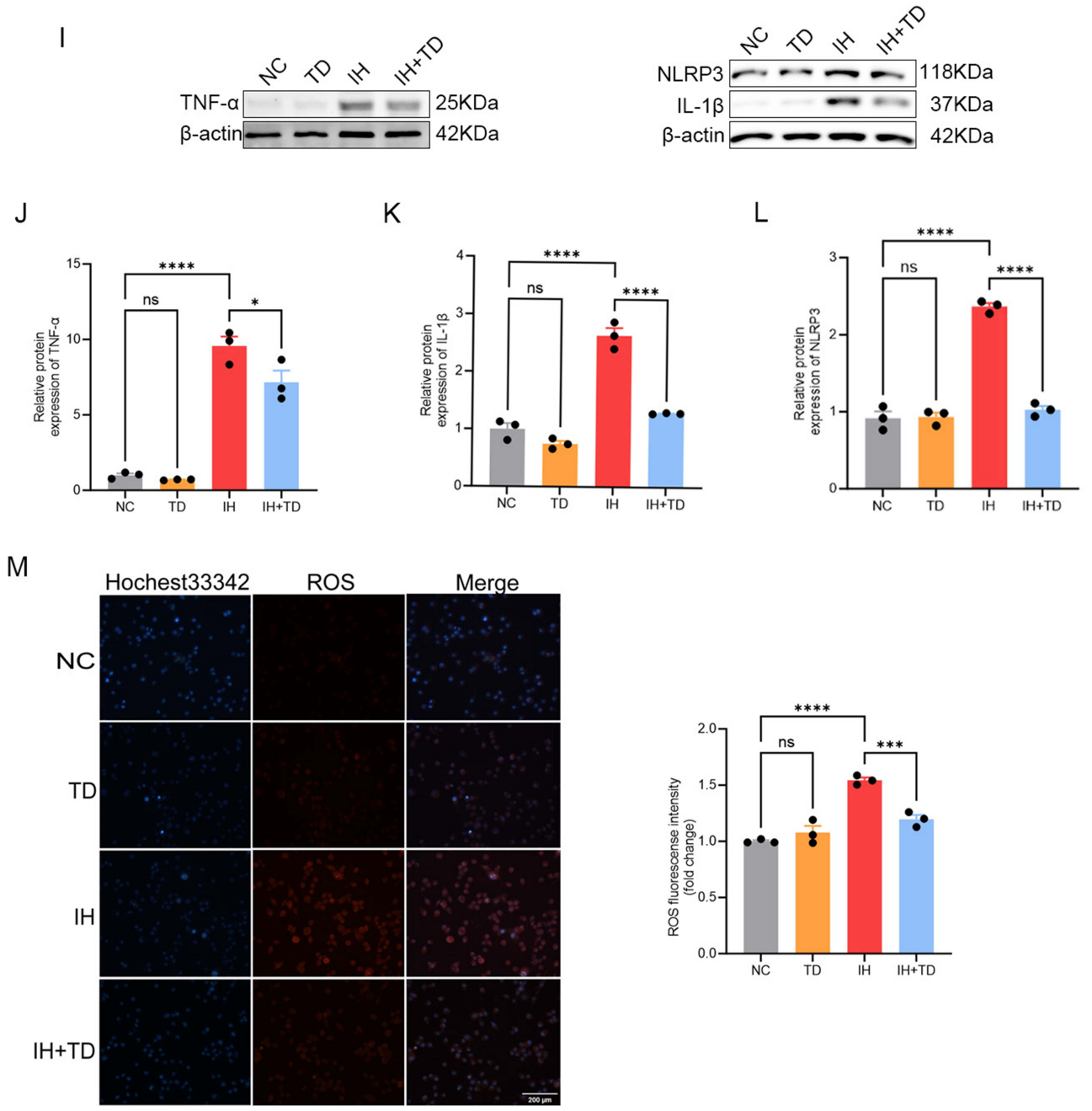

Figure 4 SET domain bifurcated histone lysine methyltransferase 1 (SETDB1) siRNA or inhibitor alleviates IH-induced activation of BV2 cells. (**A**) Protein levels of SETDB1, NLRP3, IL-1β, and TNF-α in BV2 cells determined by Western blot after SETDB1 knockdown using siRNA. Quantification of SETDB1 (**B**), NLRP3 (**C**), IL-1β (**D**), and TNF-α (**E**) protein levels. mRNA expression of TNF-α (**F**), IL-1β (**G**), and NLRP3 (**H**) detected by qRT-PCR after inhibiting SETDB1 with TD. (**I**) Protein levels of TNF-α, IL-1β, and NLRP3 detected by Western blot after treatment with the SETDB1 inhibitor TD. Corresponding quantifications shown in (**J**–**L**). (**M**) Representative immunofluorescence image of ROS (red) in BV2 cells after IH and/or TD treatment. Scale bars = 200 μm. Reactive oxygen species (ROS) intensity quantified using ImageJ. n = 3 per group. *p* values are based on one-way ANOVA. * $p < 0.05$, ** $p < 0.01$, *** $p < 0.001$ and **** $p < 0.0001$. ns = not significant.

ACE Supplementation Inhibits IH-Induced Neuroinflammation by Simultaneously Acting on NF - κB and STAT3

Given our findings that ACE supplementation might alleviate IH-induced neuroinflammation by inhibiting SETDB1, we next explored the underlying mechanisms involved. NF-κB, a critical transcription factor, is closely linked to the production of inflammatory factors such as TNF-α and IL-1β and the inflammasome NLRP3 in microglia. Previous research has shown that SETDB1 can modulate peripheral inflammatory responses through its interaction with NF-κB.[13]

https://doi.org/10.2147/JIR.S510690

In our in vitro studies, we used the inhibitor TD to block SETDB1 expression and found that p-NF-κB levels did not increase significantly following IH treatment, unlike the substantial increase observed in the IH-only treatment group compared to controls (Figure 6A and B). Additionally, we assessed the STAT3 level and its activation, another key transcription factor, and found that p-STAT3 levels significantly decreased after SETDB1 inhibition following IH stimulation ($p = 0.0051$) (Figure 6C and D).

To further investigate, we conducted in vivo studies with GTA and in vitro studies with ACE to evaluate the activation of these transcription factors. WB analysis revealed that both p-NF-κB and p-STAT3 levels were significantly reduced in the brains of mice exposed to GTA and IH compared to those exposed to IH alone (Figure 6E and F). In vitro, the IH+ACE group also showed reduced levels of p-NF-κB and p-STAT3 compared to the IH group (Figure 6G and H). These results indicate that both SETDB1 inhibition and ACE supplementation similarly affect p-NF-κB and p-STAT3 levels. Therefore, ACE's regulatory effect on IH-induced microglial inflammation likely involves modulation of the SETDB1-NF-κB-STAT3 signaling pathway.

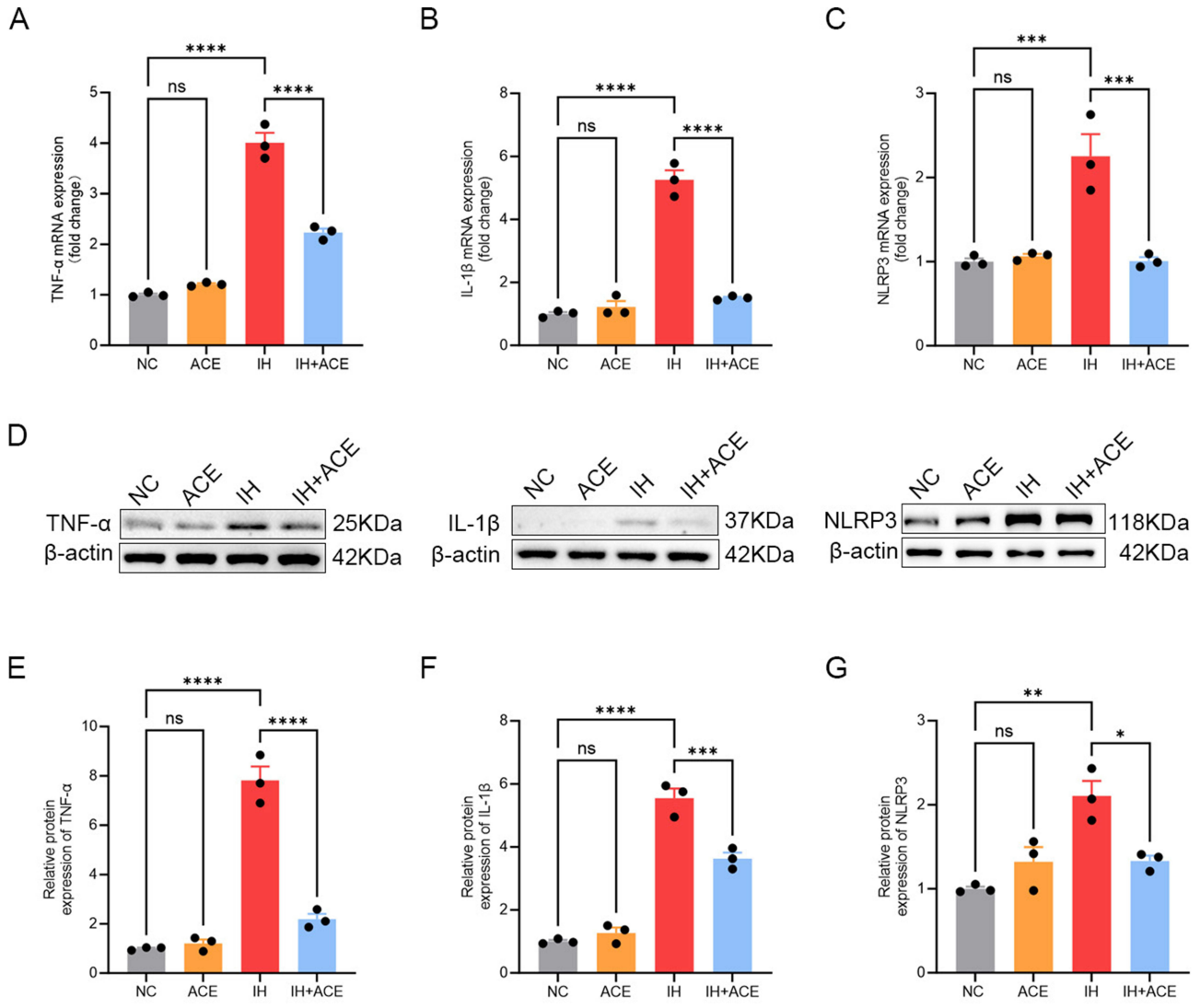

Figure 5 Continued.

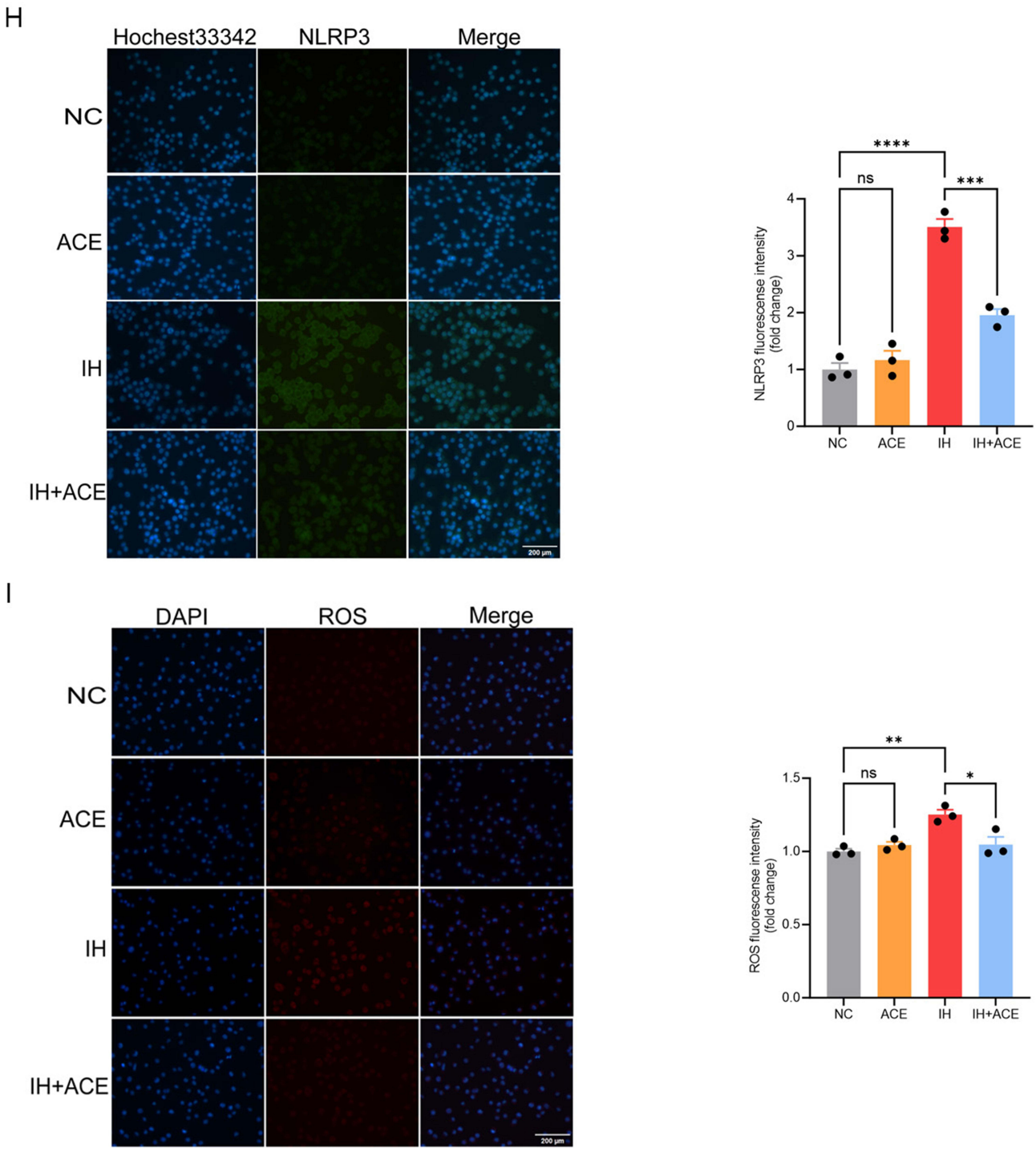

Figure 5 Acetate (ACE) alleviates IH-induced inflammatory responses in microglia in vitro. After IH and/or ACE treatment, mRNA levels of TNF-α (**A**), IL-1β (**B**) and NLRP3 (**C**) were measured by qRT-PCR in BV2 cells. (**D**) Protein levels of TNF-α, IL-1β, and NLRP3 in BV2 cells determined by Western blot, with corresponding quantifications in (**E**–**G**). Representative immunofluorescence images of NLRP3 (green) (**H**) and ROS (red) (**I**) in BV2 cells (Scale bars = 200 μm), with intensity quantified using ImageJ. n = 3 per group. The data were analyzed with one-way ANOVA. * $p < 0.05$, ** $p < 0.01$, *** $p < 0.001$ and **** $p < 0.0001$. ns = not significant.

GTA Attenuates IH-Induced Neuroinflammation and Neuronal Death

Previous studies have linked IH-associated cognitive impairment to hippocampal neuronal death. To explore whether GTA enhances cognitive function in IH mice through histological recovery, we conducted H&E staining, revealing that IH treatment led to disordered and loosely arranged neurons in the hippocampus, along with nuclear condensation and

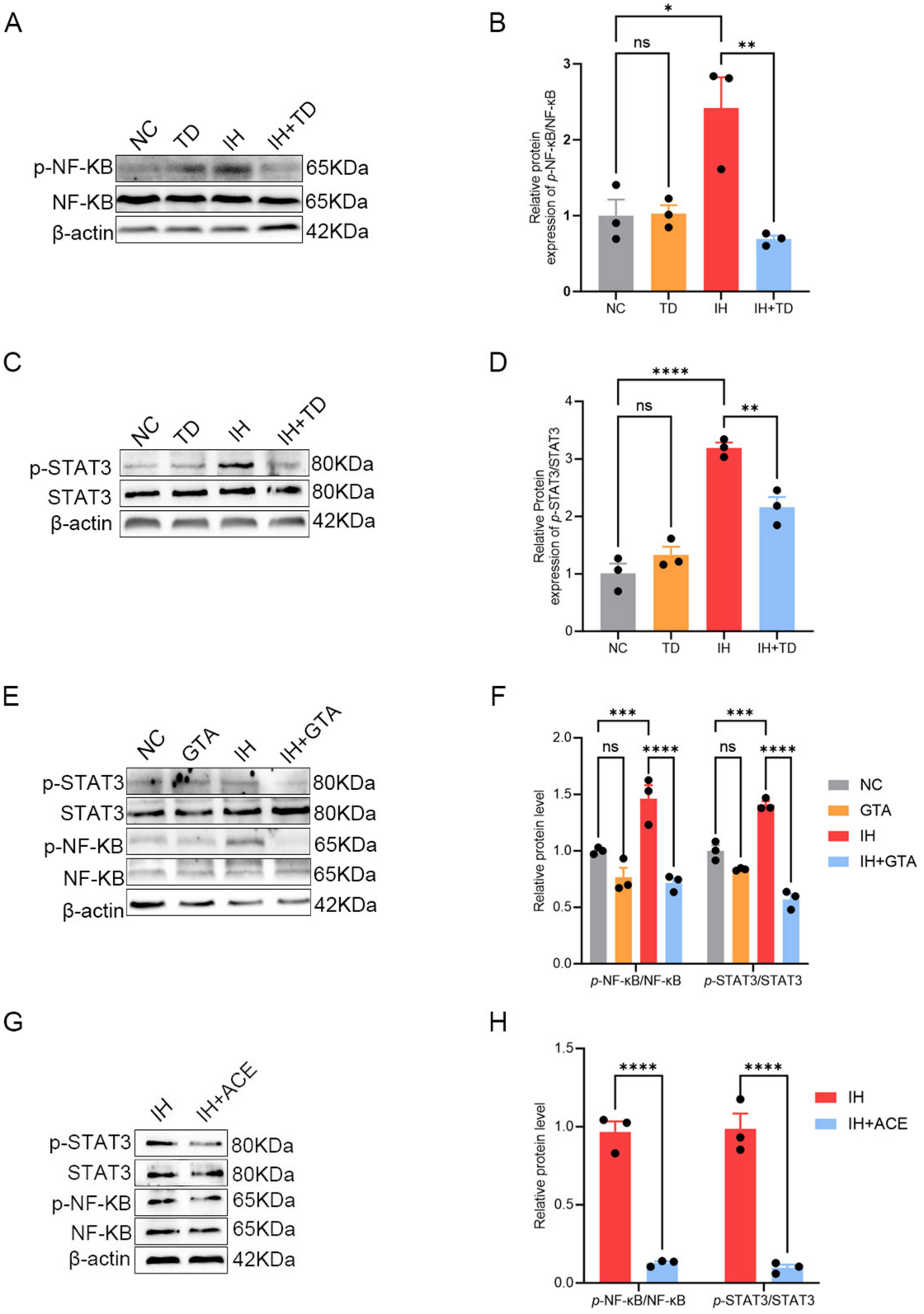

Figure 6 IH activates microglia via SET domain bifurcated histone lysine methyltransferase 1 (SETDB1) by targeting both NF-κB and signal transducer and activator of transcription 3 (STAT3) pathways. Representative Western blot images of p-NF-κB and total NF-κB (**A**), and p-STAT3 and total STAT3 (**C**) in BV2 cells treated with IH and/or TD, with quantification in (**B**) and (**D**). (**E**) In vivo glyceryl triacetate (GTA) treatment, representative Western blot images of p-STAT3, total STAT3, p-NF-κB, and total NF-κB, with quantification in (**F**). (**G**) In vitro ACE treatment, representative Western blot images of p-STAT3, total STAT3, p-NF-κB, and total NF-κB, with quantification in (**H**). *p* values are based on one-way ANOVA (**B, D** and **F**) and Student's *t* test (H). * $p < 0.05$, ** $p < 0.01$, *** $p < 0.001$ and **** $p < 0.0001$. ns = not significant.

fragmentation. However, GTA treatment significantly improved these histological abnormalities. Nissl staining of the hippocampal DG and CA1 regions showed that IH-exposed mice had a higher number of dark cells with abnormally shrunken nuclei and intense, uniform staining with cresyl violet compared to the IH+GTA group (Figure 7A, S1G). Meanwhile, for HE staining, the IH group showed neurons were arranged loosely and disorderly, some cells had nuclear pyknosis and fragmentation, and the damage was alleviated in IH+GTA group (Figure 7B). We also examined the effect of GTA on microglia activation in the hippocampus using Iba-1 immunostaining. The results indicated that Iba-1 immunoreactivity and the number of activated microglia were significantly reduced in the IH+GTA group compared to the IH group (Figure 7C, S1H). Additionally, we assessed the impact of GTA on inflammatory factors at both mRNA and protein levels. Compared to the IH group, the IH+GTA group showed a significant reduction in brain TNF-α at both mRNA and protein levels (Figure 7D–H). Likewise, GTA treatment significantly decreased elevated expressions of NLRP3 and IL-1β induced by IH (Figure 7E–H). These findings indicate that GTA has protective effects against IH-induced neuronal damage.

Discussion

OSA may lead to cognitive dysfunctions, and elucidating its pathogenesis is essential for further understanding of the disease outcomes. Here, we firstly found that ACE can effectively alleviate OSA-related cognitive dysfunction, and that could be accompanied by the inhibition of neuroinflammation and the protection of neurons. In addition, the study first discovered the pro-inflammatory effect of SETDB1 in microglia, in contrast to its anti-inflammatory effect in macrophages and revealed that ACE may improve OSA-related neuroinflammation by acting on SETDB1, thereby affecting the levels of p-STAT3 and p-NF-κB and reducing the expression of inflammatory factors.

OSA is associated with neurocognitive deficits and affects patients' quality of life.[24] Recurrent upper airway obstruction leading to IH is a significant factor contributing to pathological damage. While IH can promote nerve regeneration and reduce neuronal apoptosis,[25] the hypoxia in OSA is more severe, prolonged, and frequent compared to moderate and low-cycle IH models. In our study, mice exhibited clear neurocognitive deficits and substantial neuronal damage in the hippocampus following IH treatment. OSA exhibits distinct gender-specific patterns in both prevalence and clinical manifestations.[26] The male-to-female prevalence ratio ranges from 3:1 to 5:1, yet female appear to be more symptomatic.[27] While our study exclusively employed male mice, based on the epidemiological research on OSA, it ensures the relevance of the experimental results to the majority of affected patients to some extent. Nevertheless, the absence of female mice inevitably constrains the generalizability of our findings.

Microglia are mononuclear phagocytes of the CNS,[28] which maintains the brain homeostasis.[29] They help repair OSA-associated structural neuron damage and dysfunction at the cellular level.[30] Previous research has demonstrated that activated NF-κB signaling exacerbates neuroinflammation and contributes to cognitive dysfunction in OSA patients.[31] Consistent with these findings, our study revealed microglial activation and upregulation of NF-κB following IH exposure, along with increased levels of inflammatory mediators such as TNF-α and IL-1β. STAT3, another critical transcription factor, also showed increased activation after IH exposure in our study. Beyond its established role in the context of oncogenesis,[32] STAT3 is increasingly recognized for regulating inflammation, particularly in IL-6 signaling.[33,34] However, its function in OSA remains poorly understood. One study indicated that STAT3 activation in IH rat brains impairs learning and memory, but blocking the STAT3 signaling pathway can reverse this damage.[35]

TNF-α is crucial for initiating acute neuroinflammation,[36] while IL-1β, produced by NLRP3, is essential for transitioning from acute to chronic neuroinflammation in sepsis-related inflammation.[5] Our study observed elevated IL-1β levels compared to controls, suggesting a role in the development of OSA-related chronic neuroinflammation, warranting further investigation. Astrocytes, or glial cells, also play a significant role in neuroinflammation and may contribute to hippocampal neuronal damage induced by IH.[37] Their involvement cannot be ruled out in IH-induced neuroinflammation.

GM dysbiosis has been observed in several OSA-mimicking animal models.[38,39] Contrary to previous reports,[38,40] our IH mouse model did not show significant differences in the Chao richness, Shannon diversity and Simpson diversity between the IH and control groups, aligning with studies in OSA patients.[9] However, our taxonomic compositional analysis revealed a higher *Firmicutes*-to-*Bacteroidetes* (F/B) ratio in the IH group compared to controls. The F/B ratio's

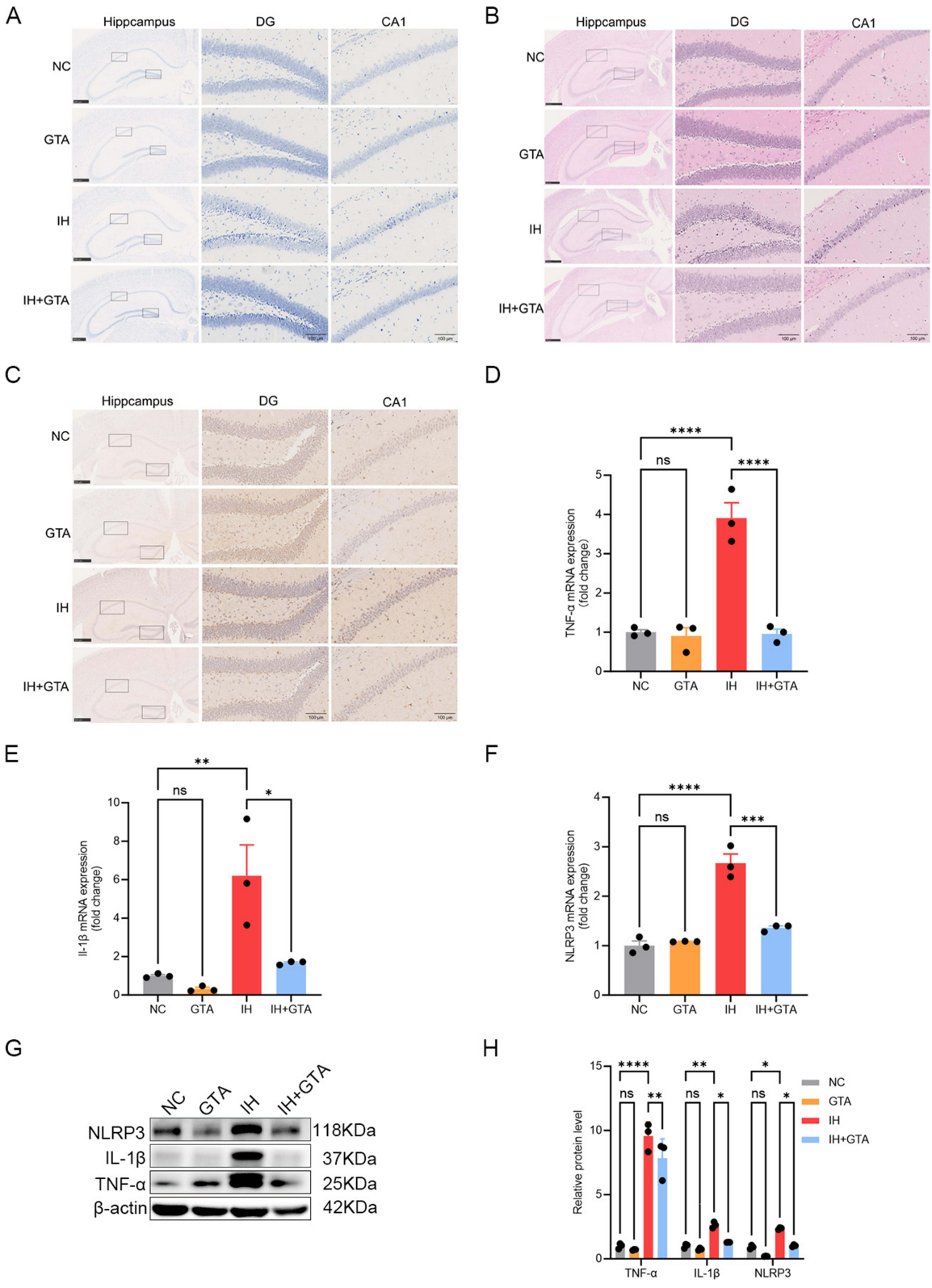

Figure 7 Glyceryl triacetate (GTA) reduces IH-induced hippocampal neuronal death in mice. (**A**) Nissl staining in the hippocampus showing necrotic cells with strong, uniform purple staining. (**B**) Representative hematoxylin and eosin (H&E) staining images of different hippocampal regions. (**C**) Immunostaining for microglial Iba-1 in the hippocampus with representative images. Scale bars = 500 μm and 100 μm. mRNA levels of TNF-α (**D**), IL-1β (**E**), and NLRP3 (**F**) detected by qRT-PCR in brain tissues. (**G**) Protein levels of TNF-α, IL-1β, and NLRP3 detected by Western blot, with β-actin as a loading control. Quantification of protein levels shown in (**H**). n = 3 per group. * $p < 0.05$, ** $p < 0.01$, *** $p < 0.001$ and **** $p < 0.0001$. ns = not significant. p values are based on one-way ANOVA.

role in neurodegenerative diseases is debated, with some studies showing a decrease in F/B in amyotrophic lateral sclerosis (ALS).[41] For the GM composition of each group, *Muribaculaceae*, dominant at the genus level in all groups, may serve as biomarkers for cognitive aging.[42] *Muribaculaceae* produces butyric acid through fermentation, which decreased after IH exposure in our study. Previous research indicated a correlation between *Muribaculaceae* and inflammatory factors in spinal cord injury studies, though this seems contrary to our findings.[43] LEfSe analysis identified *Desulfovibrio* as a marker strain of the IH group. *Desulfovibrio* abundance is linked to Parkinson's disease (PD) severity, with its metabolites potentially involved in alpha-synuclein aggregation.[44] Moreover, studies on IH have shown increased *Desulfovibrio* abundance in GM.[38]

Alongside changes in GM composition, metabolomic alterations also occur. ACE, the smallest and simplest SCFA, is known to elevate brain ACE levels.[45] GTA significantly increases ACE levels in the brain[16] and compared with direct ACE supplementation, it has higher bioavailability and maintains more stable systemic ACE concentrations.[46,47] Therefore, this study used GTA gavage to increase the level of ACE in mice brains. One study indicated that OSA significantly reduces ACE concentrations in the cecum, but not propionate or butyrate,[48] highlighting ACE's role in SCFA-mediated OSA-related diseases. We found that GTA supplementation reduced IH-induced neuroinflammation, as evidenced by decreased mRNA and protein levels of TNF-α and fewer Iba1-positive and ROS-positive cells in the hippocampus and BV2 cells, respectively. These findings support the anti-inflammatory effects of ACE observed in previous studies[49] and inflammatory bowel disease.[50,51] Acetate combines with GPR43 to alleviate perioperative neurocognitive disorders in aged mice.[52] In our study, GTA improved cognitive function, as indicated by increased spontaneous response alternation in the Y maze, more time spent in the target quadrant, and reduced escape latency in the MWM test. GTA shows human safety and an ameliorative effect on cognitive impairment related to OSA, suggesting that it may have clinical application value in the treatment of OSA.

Current research on acetate's anti-inflammatory effects often focuses on epigenetic regulation, particularly histone hyperacetylation.[53,54] For example, ACE supplementation in a rat model of LPS-induced neuroinflammation reversed decreased H3K9 acetylation and normalized IL-1β levels, reducing neuroglial activation.[55] Our study was the first to identify high SETDB1 expression in BV2 microglia cells treated with IH, with ACE reversing this elevation. Inhibiting SETDB1 through inhibitors or siRNA resulted in a significant reduction in inflammatory factors. While previous studies have linked SETDB1 to inflammation inhibition in peripheral tissues,[56] our findings suggest that SETDB1's role in the central nervous system differs. We provide new evidence that GTA alleviates IH-induced neuroinflammation by reducing SETDB1 expression. In vitro studies demonstrated that direct ACE exposure significantly downregulated SETDB1 expression, indicating its capacity to directly inhibit SETDB1. Consistent with this, in vivo studies revealed that GTA, an ACE prodrug, similarly suppressed SETDB1. For ACE can alter gut microbiota composition,[57] the potential involvement of gut microbiota changes in ACE-mediated SETDB1 regulation remains to be clarified in future. Additionally, we found that SETDB1 inhibition in BV2 cells decreased the expression of transcription factors NF-κB p65 and STAT3. Thus, ACE's mechanism for alleviating IH-induced central nervous system inflammation may involve modulation of the SETDB1-NF-κB/STAT3 signaling pathway. Notably, the effect of SETDB1 in microglia is completely opposite to that in macrophages with regard to inflammatory responses.[13] In macrophage-specific SETDB1 knockout mice, the absence of SETDB1 did not alter NF-κB p65 expression in peritoneal macrophages but increased its recruitment to pro-inflammatory factor promoters.[13] This discrepancy may arise from differences in models and immune cell types.

Limitations

This study was limited by its exclusive use of male mice, incomplete CNS cell type coverage, modest sample sizes in some cases, and lack of in vivo SETDB1 functional validation. Future work will validate SETDB1's role in vivo using conditional knockout models and increase the sample sizes. At the same time, we will incorporate both sexes, examine additional CNS cell types to perfect the mechanistic study of the ACE-SETDB1 pathway. Subsequent studies will employ precise quantitative methods to characterize neuronal injury.

Conclusions

To our knowledge, our study provides the first evidence of SETDB1's role in enhancing microglial inflammatory responses, which is in stark contrast to its function in macrophages. Furthermore, our findings highlight SETDB1's critical involvement in ACE's suppression of CNS inflammation. Additionally, our findings reveal that ACE may alleviate IH-induced cognitive dysfunction by inhibiting SETDB1, which in turn reduces the activation of STAT3 and NF-κB. These novel insights contribute to a deeper understanding of OSA-related cognitive dysfunction and ACE supplementation represents a potential nutritional therapeutic strategy for mitigating cognitive dysfunction associated with OSA.

Data Sharing Statement

The raw data supporting the conclusions of this article are available from the corresponding author on reasonable request.

Ethical Approval

All animal procedures were approved by the Animal Ethics and Laboratory Committee of Tianjin Medical University General Hospital (No, IRB2022-DW-85) and strictly adhered to the National Standard GB/T 35892-2018 (China) for Laboratory Animal Welfare.

Funding

This research was supported in part through the National Natural Science Foundation of China (82200100 to ZZ; 82170097, 81970083 to JF); as well as grants from the Tianjin Key Medical Discipline (Specialty) Construction Project (TJYXZDXK-008A).

Disclosure

The authors declare no conflicts of interest regarding the publication of this paper.

References

1. Ainge-Allen HW, Yee BJ, MSM I. Contemporary concise review 2020: sleep. *Respirology*. 2021;26(7):700–706. doi:10.1111/resp.14084
2. Bubu OM, Andrade AG, Umasabor-Bubu OQ, et al. Obstructive sleep apnea, cognition and Alzheimer's disease: a systematic review integrating three decades of multidisciplinary research. *Sleep Med Rev*. 2020;50:101250. doi:10.1016/j.smrv.2019.101250
3. Gargouri B, Yousif NM, Bouchard M, Fetoui H, Fiebich BL. Inflammatory and cytotoxic effects of bifenthrin in primary microglia and organotypic hippocampal slice cultures. *J Neuroinflammation*. 2018;15(1):159. doi:10.1186/s12974-018-1198-1
4. Block ML, Hong JS. Microglia and inflammation-mediated neurodegeneration: multiple triggers with a common mechanism. *Progress in Neurobiology*. 2005;76(2):77–98. doi:10.1016/j.pneurobio.2005.06.004
5. Zhao Z, Wang Y, Zhou R, et al. A novel role of NLRP3-generated IL-1β in the acute-chronic transition of peripheral lipopolysaccharide-elicited neuroinflammation: implications for sepsis-associated neurodegeneration. *J Neuroinflammation*. 2020;17(1):64. doi:10.1186/s12974-020-1728-5
6. Qiao Y, Wang P, Qi J, Zhang L, Gao C. TLR-induced NF-κB activation regulates NLRP3 expression in murine macrophages. *FEBS Lett*. 2012;586 (7):1022–1026. doi:10.1016/j.febslet.2012.02.045
7. Li Y, Liu M, Zuo Z, et al. TLR9 regulates the NF-κB-NLRP3-IL-1β pathway negatively in salmonella-induced NKG2D-mediated intestinal inflammation. *J Immunol*. 2017;199(2):761–773. doi:10.4049/jimmunol.1601416
8. Shi Y, Guo X, Zhang J, Zhou H, Sun B, Feng J. DNA binding protein HMGB1 secreted by activated microglia promotes the apoptosis of hippocampal neurons in diabetes complicated with OSA. *Brain Behav Immun*. 2018;73:482–492. doi:10.1016/j.bbi.2018.06.012
9. Ko CY, Liu QQ, Su HZ, et al. Gut microbiota in obstructive sleep apnea-hypopnea syndrome: disease-related dysbiosis and metabolic comorbidities. *Clin Sci*. 2019;133(7):905–917. doi:10.1042/cs20180891
10. Fusco W, Lorenzo MB, Cintoni M, et al. short-chain fatty-acid-producing bacteria: key components of the human gut microbiota. *Nutrients*. 2023;15(9). doi:10.3390/nu15092211
11. Erny D, Dokalis N, Mezö C, et al. Microbiota-derived acetate enables the metabolic fitness of the brain innate immune system during health and disease. *Cell Metab*. 2021;33(11):2260–2276.e7. doi:10.1016/j.cmet.2021.10.010
12. Markouli M, Strepkos D, Chlamydas S, Piperi C. Histone lysine methyltransferase SETDB1 as a novel target for central nervous system diseases. *Progress in Neurobiology*. 2021;200:101968. doi:10.1016/j.pneurobio.2020.101968
13. Hachiya R, Shiihashi T, Shirakawa I, et al. The H3K9 methyltransferase Setdb1 regulates TLR4-mediated inflammatory responses in macrophages. *Sci Rep*. 2016;6:28845. doi:10.1038/srep28845
14. Falkenstern L, Georgi V, Bunse S, et al. A miniaturized mode-of-action profiling platform enables high throughput characterization of the molecular and cellular dynamics of EZH2 inhibition. *Sci Rep*. 2024;14(1):1739. doi:10.1038/s41598-023-50964-x
15. Conforti F, Pala L, Di Mitri D, et al. Sex hormones, the anticancer immune response, and therapeutic opportunities. *Cancer Cell*. 2025;43(3):343–360. doi:10.1016/j.ccell.2025.02.013

16. Mathew R, Arun P, Madhavarao CN, Moffett JR, Namboodiri MA. Progress toward acetate supplementation therapy for Canavan disease: glyceryl triacetate administration increases acetate, but not N-acetylaspartate, levels in brain. *J Pharmacol Exp Ther*. 2005;315(1):297–303. doi:10.1124/jpet.105.087536
17. Miao X, Wu Q, Du S, et al. SARM1 promotes neurodegeneration and memory impairment in mouse models of alzheimer's disease. *Aging Disease*. 2024;15(1):390–407. doi:10.14336/ad.2023.0516-1
18. Lei P, Li Z, Hua Q, et al. Ursolic acid alleviates neuroinflammation after intracerebral hemorrhage by mediating microglial pyroptosis via the NF-κB/NLRP3/GSDMD pathway. *Int J mol Sci*. 2023;24(19). doi:10.3390/ijms241914771
19. Rapone R, Del Maestro L, Bouyioukos C, et al. The cytoplasmic fraction of the histone lysine methyltransferase Setdb1 is essential for embryonic stem cells. *iScience*. 2023;26(8):107386. doi:10.1016/j.isci.2023.107386
20. Qin J, Li R, Raes J, et al. A human gut microbial gene catalogue established by metagenomic sequencing. *Nature*. 2010;464(7285):59–65. doi:10.1038/nature08821
21. Robles-Vera I, Toral M, Romero M, et al. Antihypertensive effects of probiotics. *Curr Hypertens Rep*. 2017;19(4):26. doi:10.1007/s11906-017-0723-4
22. Grabrucker S, Marizzoni M, Silajdžić E, et al. Microbiota from Alzheimer's patients induce deficits in cognition and hippocampal neurogenesis. *Brain*. 2023;146(12):4916–4934. doi:10.1093/brain/awad303
23. Sawin EA, De Wolfe TJ, Aktas B, et al. Glycomacropeptide is a prebiotic that reduces Desulfovibrio bacteria, increases cecal short-chain fatty acids, and is anti-inflammatory in mice. *Am J Physiol Gastrointest Liver Physiol*. 2015;309(7):G590–601. doi:10.1152/ajpgi.00211.2015
24. Bucks RS, Olaithe M, Rosenzweig I, Morrell MJ. Reviewing the relationship between OSA and cognition: where do we go from here? *Respirology*. 2017;22(7):1253–1261. doi:10.1111/resp.13140
25. Coimbra-Costa D, Garzón F, Alva N, et al. Intermittent hypobaric hypoxic preconditioning provides neuroprotection by increasing antioxidant activity, erythropoietin expression and preventing apoptosis and astrogliosis in the brain of adult rats exposed to acute severe hypoxia. *Int J mol Sci*. 2021;22(10). doi:10.3390/ijms22105272
26. Jennum P, Riha RL. Epidemiology of sleep apnoea/hypopnoea syndrome and sleep-disordered breathing. *Europ resp J*. 2009;33(4):907–914. doi:10.1183/09031936.00180108
27. Bonsignore MR, Saaresranta T, Riha RL. Sex differences in obstructive sleep apnoea. *Eur Respir Rev*. 28(154). doi:10.1183/16000617.0030-2019
28. De Sousa RAL. Reactive gliosis in Alzheimer's disease: a crucial role for cognitive impairment and memory loss. *Metab Brain Dis*. 2022;37(4):851–857. doi:10.1007/s11011-022-00953-2
29. Kettenmann H, Kirchhoff F, Verkhratsky A. Microglia: new roles for the synaptic stripper. *Neuron*. 2013;77(1):10–18. doi:10.1016/j.neuron.2012.12.023
30. Yang Q, Wang Y, Feng J, Cao J, Chen B. Intermittent hypoxia from obstructive sleep apnea may cause neuronal impairment and dysfunction in central nervous system: the potential roles played by microglia. *Neuropsychiatr Dis Treat*. 2013;9:1077–1086. doi:10.2147/ndt.s49868
31. Dandan Z, Shen C, Liu X, Liu T, Ou Y, Ouyang R. IL-33/ST2 mediating systemic inflammation and neuroinflammation through NF-kB participated in the neurocognitive impairment in obstructive sleep apnea. *Int Immunopharmacol*. 2023;115:109604. doi:10.1016/j.intimp.2022.109604
32. Fan Y, Mao R, Yang J. NF-κB and STAT3 signaling pathways collaboratively link inflammation to cancer. *Protein & Cell Mar*. 2013;4(3):176–185. doi:10.1007/s13238-013-2084-3
33. Eskilsson A, Mirrasekhian E, Dufour S, Schwaninger M, Engblom D, Blomqvist A. Immune-induced fever is mediated by IL-6 receptors on brain endothelial cells coupled to STAT3-dependent induction of brain endothelial prostaglandin synthesis. *J Neurosci*. 2014;34(48):15957–15961. doi:10.1523/jneurosci.3520-14.2014
34. Gautron L, Lafon P, Chaigniau M, Tramu G, Layé S. Spatiotemporal analysis of signal transducer and activator of transcription 3 activation in rat brain astrocytes and pituitary following peripheral immune challenge. *Neuroscience*. 2002;112(3):717–729. doi:10.1016/s0306-4522(02)00115-x
35. Wang J, Xu Z, Xu L, Xu P. Inhibition of STAT3 signal pathway recovers postsynaptic plasticity to improve cognitive impairment caused by chronic intermittent hypoxia. *Sleep & Breathing = Schlaf & Atmung*. 2023;27(3):893–902. doi:10.1007/s11325-022-02671-6
36. Qin L, Wu X, Block ML, et al. Systemic LPS causes chronic neuroinflammation and progressive neurodegeneration. *Glia*. 2007;55(5):453–462. doi:10.1002/glia.20467
37. She N, Shi Y, Feng Y, et al. NLRP3 inflammasome regulates astrocyte transformation in brain injury induced by chronic intermittent hypoxia. *BMC neuro*. 2022;23(1):70. doi:10.1186/s12868-022-00756-2
38. Moreno-Indias I, Torres M, Montserrat JM, et al. Intermittent hypoxia alters gut microbiota diversity in a mouse model of sleep apnoea. *Europ resp J*. 2015;45(4):1055–1065. doi:10.1183/09031936.00184314
39. Poroyko VA, Carreras A, Khalyfa A, et al. Chronic sleep disruption alters gut microbiota, induces systemic and adipose tissue inflammation and insulin resistance in mice. *Sci Rep*. 2016;6:35405. doi:10.1038/srep35405
40. Farré N, Farré R, Gozal D. Sleep apnea morbidity: a consequence of microbial-immune cross-talk? *Chest*. 2018;154(4):754–759. doi:10.1016/j.chest.2018.03.001
41. Niccolai E, Di Pilato V, Nannini G, et al. The gut microbiota-immunity axis in ALS: a role in deciphering disease heterogeneity? *Biomedicines*. 2021;9(7). doi:10.3390/biomedicines9070753
42. Xia N, Xu L, Huang M, et al. Neuroprotection of macamide in a mouse model of Alzheimer's disease involves Nrf2 signaling pathway and gut microbiota. *Eur J Pharmacol*. 975:176638. doi:10.1016/j.ejphar.2024.176638
43. Rong ZJ, Cai HH, Wang H, et al. Ursolic acid ameliorates spinal cord injury in mice by regulating gut microbiota and metabolic changes. *Front Cell Neurosci*. 2022;16:872935. doi:10.3389/fncel.2022.872935
44. Murros KE, Huynh VA, Takala TM, Saris PEJ. Desulfovibrio bacteria are associated with parkinson's disease. *Front Cell Infect Microbiol*. 2021;11:652617. doi:10.3389/fcimb.2021.652617
45. Dalile B, Van Oudenhove L, Vervliet B, Verbeke K. The role of short-chain fatty acids in microbiota-gut-brain communication. *Nat Rev Gastroenterol Hepatol*. 2019;16(8):461–478. doi:10.1038/s41575-019-0157-3
46. Tsen AR, Long PM, Driscoll HE, et al. Triacetin-based acetate supplementation as a chemotherapeutic adjuvant therapy in glioma. *Int j Cancer*. 134(6):1300–1310. doi:10.1002/ijc.28465
47. Long PM, Tighe SW, Driscoll HE, et al. Acetate supplementation induces growth arrest of NG2/PDGFRα-positive oligodendroglioma-derived tumor-initiating cells. *PLoS One*. 2013;8(11):e80714. doi:10.1371/journal.pone.0080714

48. Ganesh BP, Nelson JW, Eskew JR, et al. Prebiotics, probiotics, and acetate supplementation prevent hypertension in a model of obstructive sleep apnea. *Hypertension*. 2018;72(5):1141–1150. doi:10.1161/hypertensionaha.118.11695
49. Yin X, Duan C, Zhang L, et al. Microbiota-derived acetate attenuates neuroinflammation in rostral ventrolateral medulla of spontaneously hypertensive rats. *J Neuroinflammation*. 2024;21(1):101. doi:10.1186/s12974-024-03061-3
50. Maslowski KM, Vieira AT, Ng A, et al. Regulation of inflammatory responses by gut microbiota and chemoattractant receptor GPR43. *Nature*. 7268;461:1282–1286. doi:10.1038/nature08530
51. Macia L, Tan J, Vieira AT, et al. Metabolite-sensing receptors GPR43 and GPR109A facilitate dietary fibre-induced gut homeostasis through regulation of the inflammasome. *Nat Commun*. 2015;6:6734. doi:10.1038/ncomms7734
52. Wen C, Xie T, Pan K, et al. Acetate attenuates perioperative neurocognitive disorders in aged mice. *Aging*. 12(4):3862–3879. doi:10.18632/aging.102856
53. Zhang B, West EJ, Van KC, et al. HDAC inhibitor increases histone H3 acetylation and reduces microglia inflammatory response following traumatic brain injury in rats. *Brain Res*. 2008;1226:181–191. doi:10.1016/j.brainres.2008.05.085
54. Majumdar A, Siva Venkatesh IP, Basu A. Short-chain fatty acids in the microbiota-gut-brain axis: role in neurodegenerative disorders and viral infections. *ACS Chem Neurosci*. 14(6):1045–1062. doi:10.1021/acschemneuro.2c00803
55. Soliman ML, Smith MD, Houdek HM, Rosenberger TA. Acetate supplementation modulates brain histone acetylation and decreases interleukin-1β expression in a rat model of neuroinflammation. *J Neuroinflammation*. 2012;13(9):51. doi:10.1186/1742-2094-9-51
56. Južnić L, Peuker K, Strigli A, et al. SETDB1 is required for intestinal epithelial differentiation and the prevention of intestinal inflammation. *Gut*. 2021;70(3):485–498. doi:10.1136/gutjnl-2020-321339
57. Marques FZ, Nelson E, Chu PY, et al. High-fiber diet and acetate supplementation change the gut microbiota and prevent the development of hypertension and heart failure in hypertensive mice. *Circulation*. 2017;135(10):964–977. doi:10.1161/circulationaha.116.024545